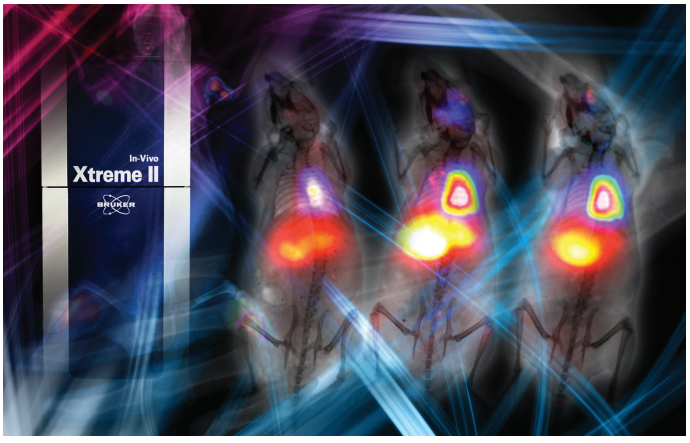

X-ray Imaging in Preclinical Studies of Bone, Pulmonary and Soft Tissues

Nikita Agarwal[1]

[1]Bruker BBIO, Preclinical Imaging, SBIC-Bruker PCI Centre, Singapore

Introduction

Discovered by Wilhelm Roentgen in 1895, X-ray technology is the oldest and most commonly used form of medical imaging and remains an important tool for the diagnosis of many disorders. X-rays are generated when a beam of electrons is accelerated by high voltage and hits a metal probe. The kinetic energy released is transformed into quanta of emitted X-ray radiation. X-rays are absorbed by the material through which they pass (interact through Compton effect, Raleigh scattering and photoelectric effect) and are affected by density of the sample. For example, bone absorption typically contrasts clearly in X-ray and is frequently shown (as with traditional film X-ray) as white areas surrounded by darker areas of tissue (Figure 1). In the body, X-ray absorption is different for bone, muscle and fat. X-ray with contrast agents also finds utility in a large number of medical applications, including angiography.

X-rays are recorded on X-ray sensitive material. Traditionally, images were obtained on photographic film, however, modern systems capture X-rays on electronic detectors and image information can be stored as a digital file for convenient use and recall. Despite development of newer technologies such as computed tomography (CT), ultrasound imaging, nuclear imaging and magnetic resonance imaging (MRI), X-ray imaging remains popular for many applications owing to the relatively fast, high-resolution imaging performance at relatively low cost. Radiography can be of 2 types: a single acquisition planar (or projection) radiography or dynamically acquired fluoroscopy. *Planar radiography*, is often applied in investigating bone health (measurement of bone density, bone fractures, etc), chest radiography (pneumonia, lung cancer), mammography (screening for breast cancer), identifying ulcers or detecting certain types of colon cancer in abdomen, intestines, liver and bladder. *Radiographic fluoroscopy* produces real-time images of internal body structure and is used to detect a number of diseases associated with the stomach and intestine, genitals and urinary tract[1,2].

Bruker Xtreme II Radiographic Modality

The Bruker In-Vivo Xtreme II system is an Optical/X-ray system offering anatomical and functional imaging modalities. The Xtreme II radiographic imaging may be used to provide anatomical reference for its functional multispectral fluorescent, bioluminescent, DRI/PET (2D), DRI/SPECT (2D) and Cherenkov modalities as shown in Figure 2, or be used as for standalone X-ray applications/imaging as shown in Figure 3.

Similar to clinical systems, In-Vivo Xtreme II radiographic capability may be applied to areas of pharmacology, bone disease (arthritis, osteoporosis, and others), metabolism, bone remodelling and others. Combined with the Bruker Bone Density Software, the density of the bone and various statistics of the size of the bone geometry can be measured. The software performs a cylindrical fitting routine to extract important parameters of selected bone segment (listed in Table 1). The algorithm models the X-ray image of a long-bone segment to a cylindrical symmetry. Based on CaPO4 immersed in water, the long-bone density measurements assume that a selected bone segment is a planar view of cylinder in a medium (as shown in Figure 4). The outer shell of the cylinder is assumed to be a homogeneous substance of higher density (bone) and the inner substance of lower density (marrow) immersed in homogenous medium of water or air[3].

For *in vivo* X-ray imaging, the subject is placed in the system Animal Management Center and atmospheric control and injection ports provide breathing mixtures and warm air for circulation from the outside of the cabinet to maintain animals during imaging. The X-ray system is optimized for small animal imaging generating voltages between 20 - 45 kVp and current maintained at 500 microamps. The micro focus X-ray imaging source control provides focal spot size of approx. 60 micron. The cone of illumination is sufficient to irradiate and measure samples within 19 cm x 19 cm area during a scan, accommodating imaging of up to 10 mice simultaneously.

Figure 1

Figure 1: Left - A representative preclinical X-ray radiograph of the mouse chest acquired by a Bruker Optical/X-ray system. Right – Bruker Multimodal In-Vivo Xtreme II system..

Figure 2

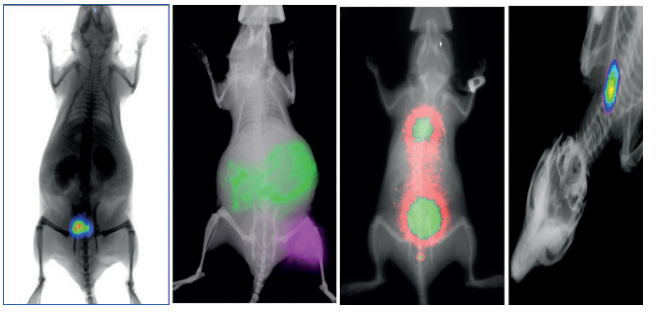

Figure 2: X-ray radiography used to reference anatomical structures for functional imaging modalities acquired sequentially with the Bruker In-Vivo Xtreme II system. From left to right – X-ray superimposed with – a bioluminescent image, a multispectral fluorescence signal, along with DRI/PET and DRI/SPECT images.

Figure 3

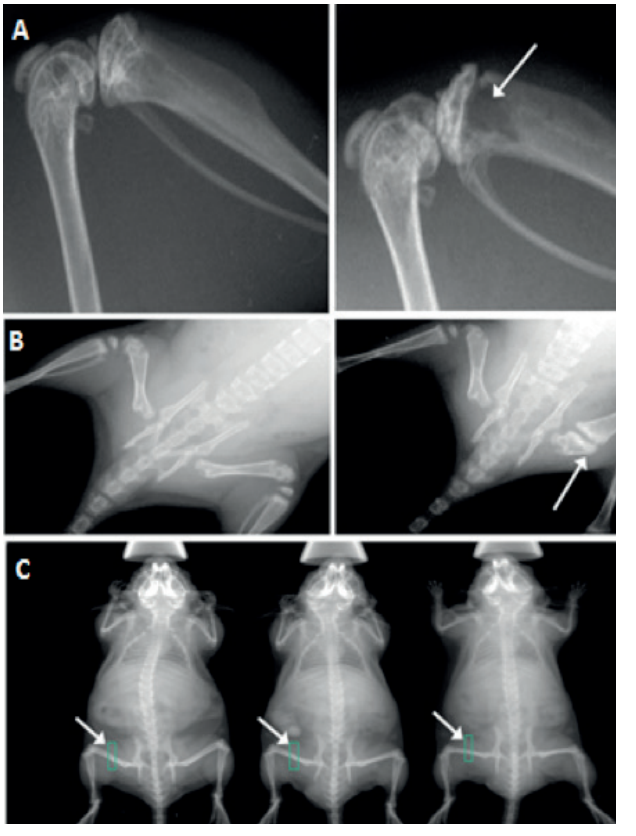

Figure 3: X-ray standalone images/applications in bone studies. Top to bottom - A) Normal (left) versus intrabone cancer (right), B) Phenotyping differences between normal (left) and knockout with disruption of the growth plate in the femur (right), and C) changes in bone density measurement simultaneously from femur of 3 mice.

Figure 4

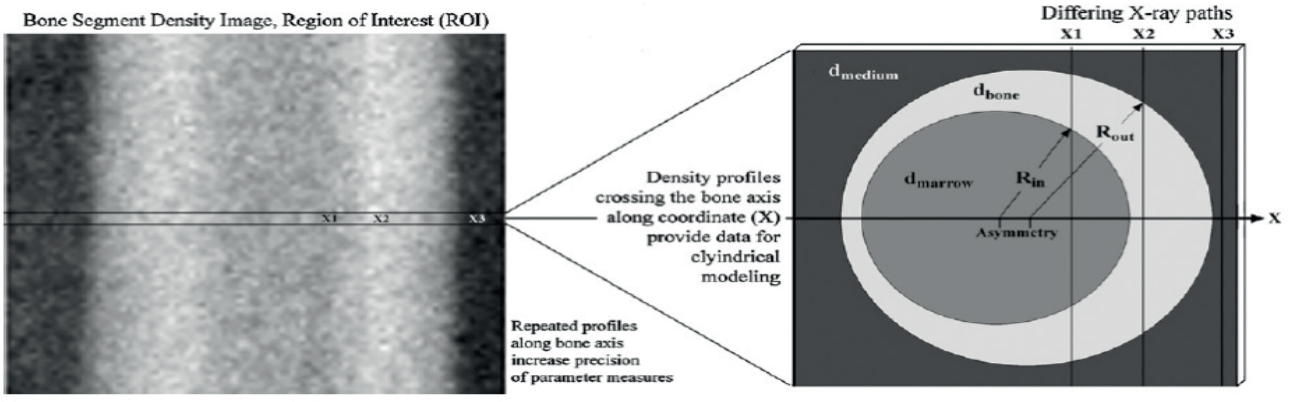

Figure 4. Non-linear least squares fitting for density measurement of cylinder bone model.

Parameters	Description
Bone or Marrow Column Density	X-ray attenuation per unit depth of material
Bone Outer and Bone Inner Radius of the long bone	Boundary between the bone and adjacent material.
Asymmetry of a long bone	Deviation between the centre of the marrow and centre of the bone cylinder (in cm)
Peripheral X-ray Density/Peripheral Depth	Thickness of tissue in which the bone is immersed. Measured density at the bone periphery. Tissue is assumed to be water and may vary from 0.2-2 cm for mouse phalange to rat femur
Water Column Density	Water equivalent column density calculated at the centre of bone
CaPO4 coefficient	Software calibrated conversion of bone column density to the volumetric density of an equivalent amount of CaPO4 in water (X-ray attenuation coefficient of calcium phosphate)
Bone Density	Bone column density corrected for the tissue depth and calibrated to CaPO4 column density. Values expressed in g/cm^3
Mean X-ray Energy	Average beam energy in the absence of a sample, taking into account attenuation of air, supporting substrates and the screen
Bone Surface Density	Average "coverage" of bone material projected back onto planar surface
Chi-Square	In non-linear least-squares fit of a cylinder to the bone segment, this value gives the robustness of fit

Table 1: List of Output Statistics of the Bruker Bone Density Software.

Figure 5

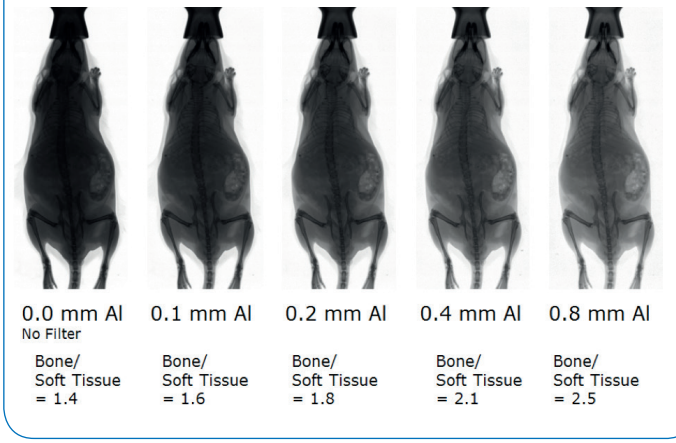

Figure 5: Mouse whole body acquisition with different beam hardening filters Al filter selected. Acquisition (125 µA) Binning 1 x 1, Exposure Time 100 s

A patented radiographic phosphor screen slides under the subject during the X-ray scan for conversion of X-ray energy to photons and detection by the cooled CCD. The system can also accommodate imaging of deep samples, including Guinea pigs and rabbits. This large depth clearance of the system is owing to the inverted design and is typically not possible with other Optical/X-ray systems (Figure 6). The system also offers a range of beam hardening aluminium filters from 0.0 mm (no filter), 0.1 mm, 0.2 mm, 0.4 mm and 0.8 mm to provide optimized contrast from soft tissues to dense tissues (Figure 5). This capability has been leveraged to investigate/measure the quantity of peripheral fat in mice and rats.

Bruker Optical/X-ray Systems and Use in X-ray Only Applications

Preclinical X-ray imaging provides innate contrast for bone, lung, and adipose tissue. The Bruker Optical/X-ray systems have been used in studies of bone disease, pulmonary disease4, and adipose measurements[5,6]. With the benefit of X-ray contrast agents soft tissue anatomy including liver, gastrointestinal tract and vasculature7 have been imaged/studied. Here, we will review select studies utilizing the X-ray imaging areas of pharmacology, bone disease and dynamic bone remodelling.

Recently, Jacqueline C. Silva et al. (2016), studied the effects of a pharmacological agent on bone density and fat deposition. Here, the authors investigated pharmacological grade Thiazolidinediones (TZDs), synthetic ligands of Peroxisome proliferator-activated receptor gamma (PPAR y). TZDs are used in clinics to treat type-2 diabetes by improving insulin resistance and controlling glycemic index. While these antidiabetic agents have benefits of improving lipid profile, endothelial dysfunction, and decreasing inflammation, they also have marked side effects such as weight gain, fluid retention, bone fractures and increased risk of cardiac failure which has led to restrictions on their use and in some cases withdrawal from the market. New drug designs to target different PPAR isotypes (dual agonists) and selective PPAR y partial agonists can offer improved therapeutic solutions. This study tests the therapeutic potential of GQ-177, a new TZD, on high fat diet induced obesity (DIO) and atherosclerosis models in low-density lipoprotein receptor-deficient (LDLr–/–) mice. Effects of GQ-177 were tested on these animals against metabolic parameters of fasting glucose and insulin, glucose tolerance and plasma lipid profile, weight gain, adipose tissue accumulation and bone density. The left femur at a specific region between the femur and hip was used for X-ray bone density analysis.

Figure 6

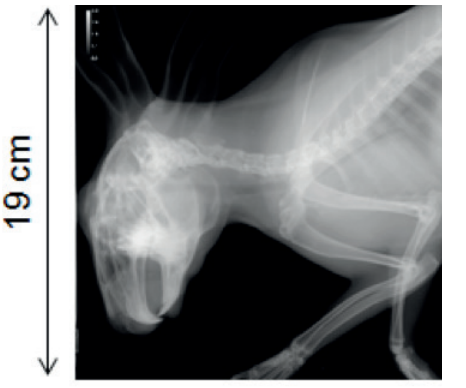

Figure 6: The Bruker Optical/X-ray systems accommodate imaging of large samples, including rabbits and large animal organs.

Additionally, a X-ray dual beam hardening method was employed to measure peripheral adipose tissue. The investigations found that the new TZD,GQ-177 drug improves insulin sensitivity and lipid profile in this animal model and X-ray bone density and adipose analysis provide physiological indicators or the possible safety profile/tolerability of the drug.

In a recent hyperhomocysteinemia study, X-ray imaging was performed with bone density analysis and vascular contrast agents (Tyagi et al., 2011). Bone degeneration occurs due to increased concentrations of homocysteine Hcy (a sulfur-containing amino acid formed in the metabolic pathway between methionine and cysteine), a state also known as hyperhomocysteinemia (HHcy) and contributes to bone abnormalities such as osteopenia and osteoporosis. Auto-oxidation of Hcy thiol groups trigger oxidative stress and increase production of reactive oxygen species (ROS). This may lead to reduced bone blood flow thereby restricting nutrient delivery to bone, endothelial dysfunction and osteoporosis. This study investigated causality between HHcy and changes in bone blood flow5. Wildtype (WT) and cystathionine-β-synthase heterozygous (CBS+/–) mice were used in this study and nutrient artery to tibia was identified using X-ray angiography (using barium sulfate contrast). Tibial bone blood flow was measured by laser doppler and ultrasonic flow probe method. Bone density (at tibia) was assessed. Interestingly, this study reported that CBS+/– mice show a decrease in bone density compared to WT. Furthermore, increased Hcy also affected vasodilatation and vasoconstriction of tibial bone nutrient artery. Folic acid treatment was administered to animals in drinking water for 6 weeks. Treatment was seen to ameliorate degeneration to some extent in CBS+/– mice compared with WT group thereby indicating that folic acid treatment may offer therapeutic potential in genetically induced HHcy bone loss.

Vijayan et al. (2013) used X-ray imaging and bone density measurements in a study of dynamic changes in bone remodelling. In conditions of postmenopause, osteoporosis and ovariectomy, estrogen levels are known to change6. Specialized bone remodelling osteoblast cells (function to produce new bone) and osteoclast cells (function to reabsorb bone) are finely regulated by RANK ligand (RANKL), a protein expressed by osteoblasts and affects osteoclast formation. Hormonal imbalances in these conditions have shown an increase in osteoclast production which adversely affects bone remodelling and leads to higher risk of bone fractures. The authors explore the role of FOXO transcription factors, mainly FOXO1, important in regulating osteoblast function. Sprague–Dawley rats were used in this experiment. Following treatment to develop higher levels of circulatory Hcy in rats, X-ray scans were acquired using the Bruker system and bone density was measured from the femur to track changes in bone integrity. The authors measure FOXO1 from femur endosteum, detect other factors such as homocysteine in serum, TRAP5b for osteoclast activity, osteoprotegerin (OPG), secreted RANKL, cytokines, osteocalcin, osteopontin and oxidative stress in bone marrow plasma. N-acetylcysteine was administered to the test subjects. N-acetylcysteine treatment was reported to decrease RANKL levels, improved bone density, cause a multi-fold decrease in serum Hcy level and decrease in osteoclast activity.

Geometric Magnification and X-ray Rotation Imaging

Special features of the Xtreme II extend the system X-ray performance/functionality. For example, the system is equipped with a magnification stage which provides 3.3 times geometric magnification offering exquisite detail particularly valuable in studies of fine structures (Figure 7A). Further, dynamic radiographic imaging is possible with Time Lapse Capture image acquisition. This function may be used in real-time for low dose scans analogous to clinical fluoroscopy or useful in multiple captures to create video files11. Combined with the unique Bruker Multimodal Animal Rotation System (MARS), an automated platform that facilitates 360° image capture, provides optimum detection of features such as fractures in bones or skull and whole body angiography as shown in Figure 7B.

Radiation Safety and Specimen Dose

Bruker Optical/X-ray systems exceed the US FDA and ASN European Safety Authority standards. System's X-ray generator is protected in a shielded enclosure and comes with safety switches, status indicators and an external software interface. A manual emergency shutoff switch and Key Control is included. Electromechanical interlocks are configured in the doors and installation components to restrict activity to only when the system is properly installed and the cabinet door is closed. Routine X-ray imaging is short (1.2 sec) and produce a dose (~0.3mGy) significantly lower than even the typically lowest resolution microCT imaging

Conclusions

The Bruker In-Vivo Xtreme II provides multimodal Optical/X-ray imaging. Combined with functional imaging, X-ray imaging can provide a valuable anatomical map. The X-ray imaging has also been employed in several anatomical studies of bone and soft tissue disease frequently employing the available advanced features including beam hardening, bone density analysis, geometric magnifications, and large sample depth imaging, only available with the Bruker In-Vivo Optical/X-ray systems.

Figure 7

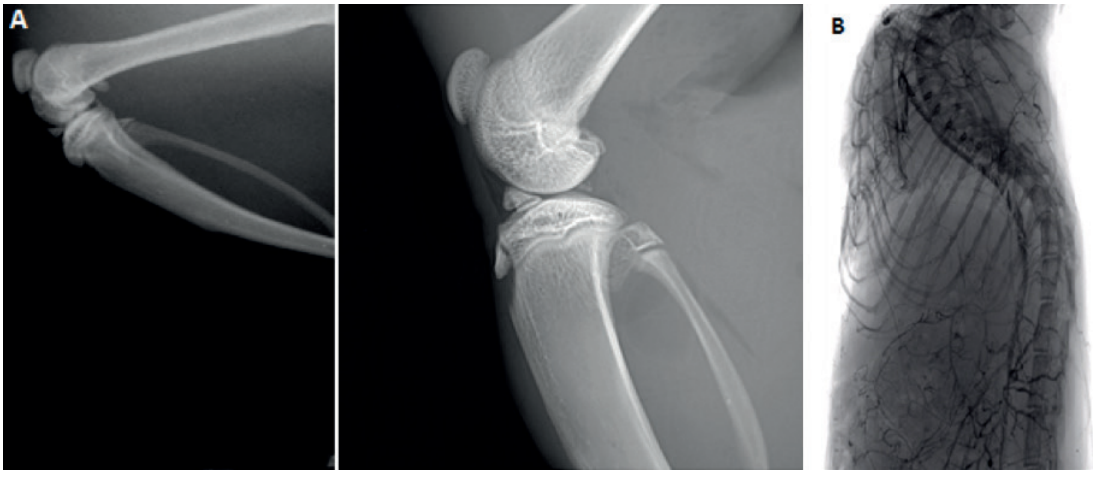

Figure 7: A) Radiographic image without magnification (left) with geometric magnification (right).
B) Single projection of whole body angiography using MARS rotation. Rotation video can be viewed at: https://youtu.be/13Kd6iBKWVU

References

[1] Medical Imaging Modalities « MITA. Available at: http://www.medicalimaging.org/ABOUT-MITA/MEDICAL-IMAGING-PRIMER/#X-RAY. (Accessed: 1st August 2016)

[2] Radiography (Plain X-rays). Understanding Medical Radiation Available at: http://www.medicalradiation.com/types-of-medical-imaging/imaging-using-X-rays/radiography-plain-X-rays/. (Accessed: 1st August 2016)

[3] Vizard, D. L. et al. Analytical radiography for planar radiographic images implemented with a multi-modal system. Comput. Methods Programs Biomed. 99, 88–97 (2010).

[4] Gammon, S.T. et al. Preclinical anatomical, molecular, and functional imaging of the lung with multiple modalities. Am J Physiol Lung Cell Mol Physiol. 306. L897-L914 (2014)

[5] Chapman, S.E. et al. Dual energy X-ray method for direct visualization and quantitative measurement of peripheral adipose in small animals. Bruker Application Note AP0103. (2011)

[6] Relationship between protein intake and weight gain. Available at: http://www.usp.br/aun/exibir.php?id=7617 (Accessed: 1st August 2016).

[7] Silva, J. C. et al. New PPARγ partial agonist improves obesity-induced metabolic alterations and atherosclerosis in LDLr(-/-) mice. Pharmacol. Res. 104, 49–60 (2016).

[8] Givvimani, S.et al. X-ray imaging of differential vascular density in MMP-9-/-, PAR-1-/+, hyperhomocysteinemic CBS-/+) and diabetic (Ins2-/+) mice. Arch. Physiol Biochem. 117, 1-7.

[9] Tyagi, N. et al. Homocysteine mediated decrease in bone blood flow and remodeling: role of folic acid. J. Orthop. Res. Off. Publ. Orthop. Res. Soc. 29, 1511–1516 (2011).

[10] Vijayan, V. et al. Homocysteine alters the osteoprotegerin/RANKL system in the osteoblast to promote bone loss: pivotal role of the redox regulator forkhead O1. Free Radic. Biol. Med. 61, 72–84 (2013).

[11] Orton, S. et al. Dynamic X-ray Imaging of Iodinated Contrast-Agent Clearance

[12] From a Living Mouse. Bruker Application Note AP0101 (2010)

Bruker BioSpin

info@bruker.com
www.bruker.com